Ultrahigh-Energy Neutrino-Nucleon Deep-Inelastic Scattering and the Froissart Bound

Alexey Yu. Illarionov,[1] Bernd A. Kniehl,[2] and Anatoly V. Kotikov[2,3]

[1]*Dipartimento di Fisica dell'Universitá di Trento, via Sommarive 14, 38050 Povo, Trento, Italy*
[2]*II. Institut für Theoretische Physik, Universität Hamburg, Luruper Chaussee 149, 22761 Hamburg, Germany*
[3]*Bogoliubov Laboratory for Theoretical Physics, JINR, 141980 Dubna (Moscow region), Russia*

(Received 18 February 2011; published 10 June 2011)

We present a simple formula for the total cross section $\sigma^{\nu N}$ of neutral- and charged-current deep-inelastic scattering of ultrahigh-energy neutrinos on isoscalar nuclear targets, which is proportional to the structure function $F_2^{\nu N}(M_V^2/s, M_V^2)$, where M_V is the intermediate-boson mass and s is the square of the center-of-mass energy. The coefficient in front of $F_2^{\nu N}(x, Q^2)$ depends on the asymptotic low-x behavior of $F_2^{\nu N}$. It contains an additional $\ln s$ term if $F_2^{\nu N}$ scales with a power of $\ln(1/x)$. Hence, an asymptotic low-x behavior $F_2^{\nu N} \propto \ln^2(1/x)$, which is frequently assumed in the literature, already leads to a violation of the Froissart bound on $\sigma^{\nu N}$.

DOI: 10.1103/PhysRevLett.106.231802 PACS numbers: 13.15.+g, 13.85.Hd, 25.30.Pt, 95.85.Ry

For more than a decade, large experiments have been searching for ultrahigh-energy (UHE) cosmic neutrinos (ν), with energies $E_\nu > 10^6$ GeV, by using detectors scanning for events in large volumes of water, ice, Earth's atmosphere, and lunar regolith [1]. While no clear indication of such an event has yet been reported, experimental bounds on UHE-neutrino fluxes could be established, which, put together, now cover energies way up to 10^{12} GeV and start to constrain scenarios of astrophysical interest. Since these limits directly depend on the total cross section $\sigma^{\nu N}(E_\nu)$ of UHE-neutrino deep-inelastic scattering (DIS) off nucleons (N), it is an urgent task to provide reliable theoretical predictions for the latter in the asymptotic high-E_ν regime, which lies far beyond the one explored by laboratory-based νN DIS experiments and corresponds to asymptotically low values of Bjorken's scaling variable x. This requires extrapolation over several orders of magnitude in E_ν, for which various approaches exist [2–8]. These are based on successful descriptions of the terrestrial data within the framework of perturbative QCD and frequently impose the Froissart bound [9] on $\sigma^{\nu N}$. According to the latter, unitarity and analyticity limit the total cross section of a scattering process not to grow faster with energy than $\ln^2 s$.

In this Letter, we derive a general formula for $\sigma^{\nu N}$ that is remarkably concise and correctly accounts for the asymptotic high-energy behavior, making it perfectly suitable for UHE-neutrino phenomenology. It is proportional to the DIS structure function $F_2^{\nu N}(x, Q^2)$, which has a well-known representation in terms of parton distribution functions (PDFs) within the parton model (PM) of QCD, with x and the typical energy scale Q appropriately defined in terms of E_ν and M_V ($V = W, Z$). To be on the conservative side, we assume for the time being, as in Refs. [2–8], that the available experimental data on DIS allow for an extrapolation to very high (low) values of E_ν (x) using an appropriate parameterization of $F_2^{\nu N}$. If the latter rises too steeply as $x \to 0$, then possible new QCD phenomena, such as gluon saturation or recombination, color glass condensates, multiple Pomeron exchanges, etc., are expected to enter the stage as a cure at x values below those currently probed by DIS experiments (for a review, see Ref. [10]). We shall return to this issue below, considering two popular models of screening [11,12].

Specifically, we consider the charged-current (CC) and neutral-current (NC) DIS processes

$$\begin{aligned} \nu(k) + N(P) &\to \ell(k') + X, \\ \nu(k) + N(P) &\to \nu(k') + X, \end{aligned} \tag{1}$$

respectively, where $N = (p + n)/2$ denotes an isoscalar nucleon target of mass M, X collects the unobserved part of the final state, and the four-momentum assignments are indicated in parentheses, and introduce the familiar kinematic variables

$$s = (k + P)^2, \quad Q^2 = -q^2, \quad x = \frac{Q^2}{2q \cdot P}, \quad y = \frac{q \cdot P}{k \cdot P}, \tag{2}$$

where $q = k - k'$. In the target rest frame, we have $s = M(2E_\nu + M)$ and $xy = Q^2/(2ME_\nu)$. In the kinematic regime of interest here, the inclusive spin-averaged double-differential cross sections of processes (1) are, to a very good approximation, given by [3]

$$\frac{d^2\sigma_i^{\nu N}}{dxdy} = \frac{G_F^2 M E_\nu}{2\pi} K_i \left(\frac{M_V^2}{Q^2 + M_V^2}\right)^2 K(y) F_2^{\nu N}, \tag{3}$$

where $i = \mathrm{CC}, \mathrm{NC}$, G_F is Fermi's constant, and $K(y) = 2 - 2y + y^2$. In the so-called *wee parton* picture appropriate for the low-x regime [7], we have $K_{\mathrm{CC}} = 1$ and $K_{\mathrm{NC}} = 1/2 - x_w + (10/9)x_w^2$, where $x_w = \sin^2\theta_w$, with θ_w being the weak mixing angle. Using $x_w = 0.231$ [13], we have $K_{\mathrm{NC}} = 0.328$. The contributions due to the structure functions $F_L^{\nu N}$ and $F_3^{\nu N}$ to the right-hand side (rhs) of

Eq. (3) are negligibly small in our applications; $F_L^{\nu N}$ tends to zero as Q^2 rises [14], and $F_3^{\nu N}$ essentially refers to valence partons, which hardly contribute in the low-x regime.

Detailed inspection of the available ℓN DIS data (see, e.g., Fig. 1 for ep data from HERA I [15]) suggests that, in the limit $x \to 0$, $F_2^{\ell N}$ exhibits a singular behavior of the form $F_2^{\ell N}(x, Q^2) \simeq x^{-\delta} \tilde{F}_2^{\ell N}(x, Q^2)$, where δ is a small positive number and $\tilde{F}_2^{\ell N}$ diverges less strongly than any power of x, i.e., $\tilde{F}_2^{\ell N}(x, Q^2)/x^{-\lambda} \to 0$ as $x \to 0$ for any positive number λ. Assuming a symmetric quark sea, as is appropriate for the low-x regime, we have $F_2^{\nu N}(x, Q^2) = (18/5)F_2^{\ell N}(x, Q^2)$, so that the low-$x$ behavior of $\tilde{F}_2^{\ell N}$ carries over to $\tilde{F}_2^{\nu N}$.

Imposing the lower cutoff Q_0^2 on Q^2, the total cross sections of processes (1) are evaluated as

$$\sigma_i^{\nu N}(E_\nu) = \frac{1}{2ME_\nu} \int_{Q_0^2}^{2ME_\nu} dQ^2 \int_{\hat{x}}^1 \frac{dx}{x} \frac{d^2\sigma_i^{\nu N}}{dxdy}, \quad (4)$$

where $\hat{x} = Q^2/(2ME_\nu)$. By inserting Eq. (3), Eq. (4) becomes

$$\sigma_i^{\nu N}(E_\nu) = \frac{G_F^2}{4\pi} K_i \int_{Q_0^2}^{2ME_\nu} dQ^2 \left(\frac{M_V^2}{Q^2 + M_V^2}\right)^2 \times \int_{\hat{x}}^1 \frac{dx}{x} K\left(\frac{\hat{x}}{x}\right) F_2^i(x, Q^2). \quad (5)$$

The inner integral on the rhs of Eq. (5) can be rewritten as the Mellin convolution $K(\hat{x}) \otimes F_2^{\nu N}(\hat{x}, Q^2)$. By exploiting the low-$x$ asymptotic form $F_2^{\nu N}(x, Q^2) \simeq x^{-\delta} \tilde{F}_2^{\nu N}(x, Q^2)$ explained above, this Mellin transform may be represented, at small values of $\hat{x}$, in the factorized form $\tilde{M}(\hat{x}, Q^2, 1 + \delta) F_2^{\nu N}(\hat{x}, Q^2)$ up to terms of $\mathcal{O}(\hat{x})$ [16]. Here,

$$\tilde{M}(\hat{x}, Q^2, 1 + \delta) = 2\left(\frac{1}{\tilde{\delta}(\hat{x}, Q^2)} - \frac{1}{\delta}\right) + M(1 + \delta), \quad (6)$$

$$\frac{1}{\tilde{\delta}(x, Q^2)} = \frac{1}{\tilde{F}_2^{\nu N}(x, Q^2)} \int_x^1 \frac{dy}{y} \tilde{F}_2^{\nu N}(y, Q^2), \quad (7)$$

$$M(n) = \int_0^1 dx x^{n-2} K(x) = \frac{2}{n-1} - \frac{2}{n} + \frac{1}{n+1}. \quad (8)$$

Hence, Eq. (5) becomes

$$\sigma_i^{\nu N}(E_\nu) \simeq \frac{G_F^2}{4\pi} K_i \int_{Q_0^2}^{2ME_\nu} dQ^2 \left(\frac{M_V^2}{Q^2 + M_V^2}\right)^2 \times \tilde{M}(\hat{x}, Q^2, 1 + \delta) F_2^{\nu N}(\hat{x}, Q^2). \quad (9)$$

Because the Q^2 dependence of $F_2^{\nu N}(\hat{x}, Q^2)$ and hence $\tilde{M}(\hat{x}, Q^2, 1 + \delta)$ is only logarithmic, the factor $[M_V^2/(Q^2 + M_V^2)]^2$ essentially fixes the scale $Q^2 = M_V^2$ [5], so that Eq. (9) simplifies to

$$\sigma_i^{\nu N}(E_\nu) \simeq \frac{G_F^2}{4\pi} K_i M_V^2 \tilde{M}(\tilde{x}, M_V^2, 1 + \delta) F_2^{\nu N}(\tilde{x}, M_V^2), \quad (10)$$

where $\tilde{x} = M_V^2/(2ME_\nu)$. This is our master formula. Further simplification depends on the actual size of δ, and we distinguish two cases. (i) If δ is not too small, so that $\hat{x}^\delta \ll$ const, then the lower limit $\hat{x}$ of the inner integral on the rhs of Eq. (5) may be put to zero, so that

$$\tilde{M}(\hat{x}, Q^2, 1 + \delta) = M(1 + \delta) = \frac{4 + 3\delta + \delta^2}{\delta(\delta + 1)(\delta + 2)} \quad (11)$$

becomes independent of $\hat{x}$ and Q^2. (ii) On the other hand, if $\delta \ll 1$, then we have

$$\tilde{M}(\hat{x}, Q^2, 1 + \delta) = \tilde{M}(\hat{x}, Q^2, 1) = \frac{2}{\tilde{\delta}(\hat{x}, Q^2)} - \frac{3}{2}. \quad (12)$$

We note that $\tilde{\delta}$ is determined by the asymptotic low-x behavior of $\tilde{F}_2^{\nu N}$. For instance, if $\tilde{F}_2^{\nu N}(x, Q^2) \propto \ln^p(1/x)$ for $x \to 0$, then $1/\tilde{\delta}(x, Q^2) = \ln(1/x)/(p + 1)$ [17].

Now we apply Eq. (10) to the three most popular types of $F_2^{\ell N}$ parameterization, namely, the standard PM representation implemented with up-to-date proton PDFs [15,18,19], a modification of the impressively simplistic log-log form proposed by Haidt (H) [20], and the more sophisticated form recently introduced by Berger, Block, and Tan (BBT) [6]. While the Q^2 dependence of the PM representation of $F_2^{\nu N}$ is governed by the Dokshitzer-Gribov-Lipatov-Altarelli-Parisi evolution, those of the heuristic H and BBT forms are directly determined by global fits to experimental data covering a wide Q^2 range. In the low-x regime, the PM parameterization of $F_2^{\ell N}$ may be well approximated by the following ansatz:

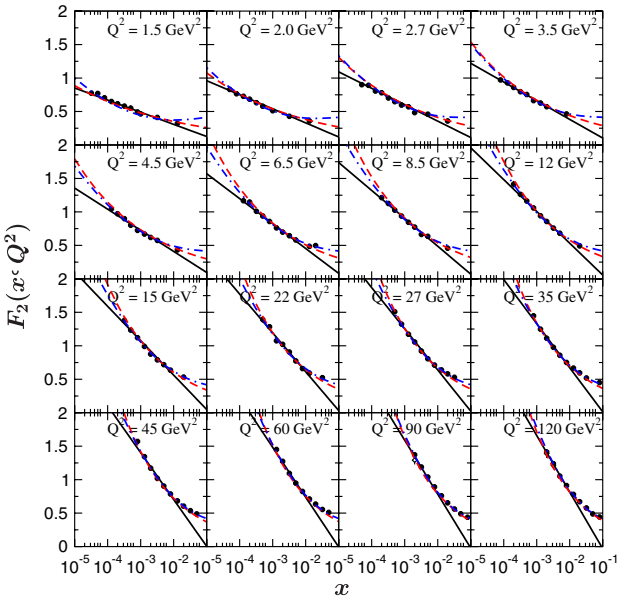

FIG. 1 (color online). Measurement of $F_2^{\ell N}$ [15] compared with our fit using the improved H ansatz as well as the PM and BBT results.

$$F_{2,\mathrm{PM}}^{\ell N}(x,Q^2) = C_{\mathrm{PM}}(Q^2)x^{-\delta_{\mathrm{PM}}(Q^2)}, \tag{13}$$

$$C_{\mathrm{PM}}(Q^2) = c_0 + c_1 \ln Q^2 + c_2 \ln^2 Q^2, \tag{14}$$

$$\delta_{\mathrm{PM}}(Q^2) = \delta_0 + \delta_1 \ln Q^2 + \delta_2 \ln^2 Q^2, \tag{15}$$

where it is understood that Q^2 is taken in units of GeV^2. To suppress higher-twist effects, we impose the cut $Q^2 > 3.5\ \mathrm{GeV}^2$. Fitting Eqs. (13)–(15) to the result for $F_2^{\ell N}$ evaluated at next-to-leading order with the HERAPDF1.0 [15] proton PDFs, we obtain the values of c_i and δ_i collected in Table I. From Eq. (15) and Table I, we glean that

$$\delta_{\mathrm{PM}}(M_Z^2) \approx \delta_{\mathrm{PM}}(M_W^2) \approx 0.37, \tag{16}$$

so that Eq. (10) is to be used with Eq. (11). Using the Martin-Stirling-Thorne-Watt [18] and coordinated theoretical-experimental project on QCD [19] PDFs, we obtain $\delta_{\mathrm{PM}}(M_V^2) \approx 0.35$ and 0.38, respectively. The resulting high-E_ν behavior $\sigma_i^{\nu N}(E_\nu) \propto \tilde{x}^{-\delta_{\mathrm{PM}}(M_V^2)}$ is in good agreement with other studies [4].

For the reader's convenience, we recollect here the BBT parameterization of $F_2^{\ell N}$ appropriate for the range $x < x_P = 0.11$ [8] relevant for our applications [6–8]:

$$F_{2,\mathrm{BBT}}^{\ell N}(x,Q^2) = (1-x)\Big[A_0 + A_1(Q^2)\ln\frac{x_P(1-x)}{x(1-x_P)} + A_2(Q^2)\ln^2\frac{x_P(1-x)}{x(1-x_P)}\Big], \tag{17}$$

where $A_0 = F_P/(1-x_P)$, with $F_P = 0.413$ [8], and

$$A_i(Q^2) = a_{i0} + a_{i1}\ln Q^2 + a_{i2}\ln^2 Q^2 \qquad (i = 1, 2), \tag{18}$$

with the values of a_{ij} listed in Table I [8]. Here, Eq. (10) is to be used with Eq. (12), and we find

$$\frac{1}{\tilde{\delta}_{\mathrm{BBT}}(x,Q^2)} \simeq \frac{\sum_{i=0}^2 A_i \ln^{i+1}(x_P/x)/(i+1)}{\sum_{i=0}^2 A_i \ln^i(x_P/x)} \simeq \frac{1}{3}\ln\frac{x_P}{x}. \tag{19}$$

From Eqs. (17) and (19), we glean that, in the high-energy limit $s \to \infty$, $F_{2,\mathrm{BBT}}^{\ell N}(\tilde{x}, M_V^2) \propto \ln^2 s$ and $1/\tilde{\delta}_{\mathrm{BBT}}(\tilde{x}, M_V^2) \propto \ln s$. This leads us to the important observation that $\sigma_{\mathrm{BBT}}^{\nu N} \propto \ln^3 s$, which manifestly violates the Froissart bound [9] in contrast to what is stated in Refs. [6–8]. This violation of the Froissart bound is attributed to the presence of the $\ln^2 x$ term in Eq. (17). On the other hand, if $F_2^{\ell N}$ just rises linearly in $\ln x$ as $x \to 0$, then $\sigma_i^{\nu N} \propto \ln^2 s$ in accordance with the Froissart bound.

TABLE I. The values of the fit parameters appearing in Eqs. (14), (15), (18), and (20).

i	$c_i \times 10^3$	$\delta_i \times 10^2$	$a_{1i} \times 10^2$	$a_{2i} \times 10^3$	$b_i \times 10^2$
0	189.4	10.90	−8.471	12.92	2.689
1	1.811	6.249	4.190	0.2473	11.63
2	−0.6054	−0.3722	−0.3976	1.642	−0.7307

In fact, this is the case for the original H ansatz [20], $B\ln(x_0/x)\ln(1+Q^2/Q_0^2)$, which contains just three fit parameters. To enable the fit quality to be improved, we introduce three more parameters by writing

$$F_{2,\mathrm{H}}^{\ell N}(x,Q^2) = B_0 + B_1(Q^2)\ln\frac{x_0}{x}, \qquad B_1(Q^2) = \sum_{i=0}^{2} b_i \ln^i\Big(1+\frac{Q^2}{Q_0^2}\Big). \tag{20}$$

Equation (10) is again to be used with Eq. (12), and we obtain

$$\frac{1}{\tilde{\delta}_{\mathrm{H}}(x,Q^2)} \simeq \frac{\sum_{i=0}^1 B_i \ln^{i+1}(x_0/x)/(i+1)}{\sum_{i=0}^1 B_i \ln^i(x_0/x)} \simeq \frac{1}{2}\ln\frac{x_0}{x}, \tag{21}$$

so that $\sigma_{\mathrm{H}}^{\nu N} \propto \ln^2 s$ as it should. Fitting Eq. (20) to the recent combination of the complete H1 and ZEUS data sets on $F_2^{\ell N}$ from HERA I [15] with the cuts $x < 0.01$ and $Q^2 > 1.5\ \mathrm{GeV}^2$, we obtain $x_0 = 0.05791$, $Q_0^2 = 2.578\ \mathrm{GeV}^2$, $B_0 = 0.1697$, and the values of b_i listed in Table I, with $\chi^2/\mathrm{d.o.f.} = 422/175 \approx 2.41$.

Looking at Fig. 1, we observe that our fit (solid lines) indeed yields a surprisingly good description of the experimental data over the full x and Q^2 ranges considered. The approximation works particularly well for low x and large Q^2 values and is thus likely to allow for a reliable extrapolation to the x and Q^2 ranges relevant for UHE-neutrino physics. In fact, switching to the cut $x < 10^{-3}$ reduces $\chi^2/\mathrm{d.o.f.}$ by roughly a factor of 3, to $\chi^2/\mathrm{d.o.f.} = 58/69 \approx 0.84$. For comparison, also the PM results evaluated from Eqs. (13)–(15) (dashed lines) and the BBT results evaluated from Eqs. (17) and (18) (dash-dotted line), which are hardly distinguishable from one another, are shown in Fig. 1.

We now consider νN DIS with UHE neutrinos. For the sake of brevity, we focus our attention on CC DIS. The corresponding NC results may be obtained by substituting $K_{\mathrm{CC}} \to K_{\mathrm{NC}}$ and $M_W \to M_Z$ in our formulas. In order to determine the range of validity of our master formula (10) for $\sigma_{\mathrm{CC}}^{\nu N}$, we compare it with the exact formula (5), which requires two-dimensional numerical integration, for the PM, BBT, and H cases considered above. In each case, we find excellent agreement for E_ν values of the order of 10^7 GeV and above, which corresponds to x values of the order of 10^{-3} and below in $F_2^{\ell N}$. This is illustrated for the BBT case in Fig. 2, where the approximate evaluation of Eq. (10) with Eqs. (12) and (19) is compared with the exact one of Eq. (5) with Eqs. (17) and (18) (dashed line). The large-E_ν approximation may be somewhat improved by evaluating $\tilde{\delta}(x,Q^2)$ by one-dimensional integration via Eq. (7) instead of using Eq. (19) (dotted line).

The PM and H results for $\sigma_{\mathrm{CC}}^{\nu N}$ evaluated from our master formula (10), with Eqs. (11) and (16) in the PM case and with Eqs. (12) and (21) in the H case, are also displayed in Fig. 2. Comparing them with the corresponding BBT result, we observe that all three predictions agree relatively well in the range $10^7\ \mathrm{GeV} \lesssim E_\nu \lesssim 10^9\ \mathrm{GeV}$, where the

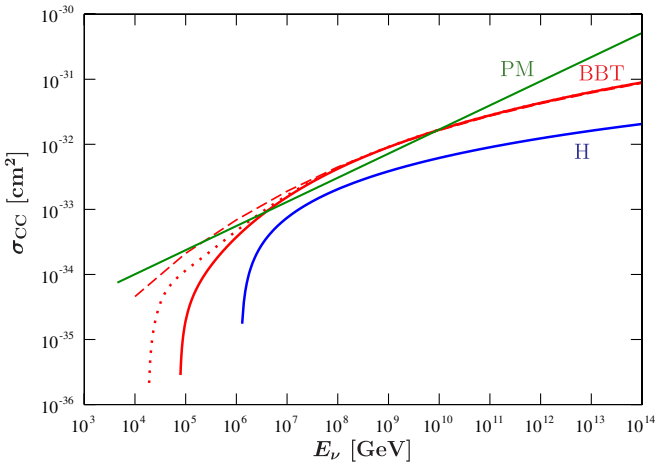

FIG. 2 (color online). Predictions for $\sigma_{CC}^{\nu N}(E_\nu)$ evaluated from the PM, BBT, and H parameterizations of $F_2^{\ell N}(x, Q^2)$. In the BBT case, also the improved high-E_ν approximation and the exact evaluation are shown.

high-E_ν approximation is already working and the respective $F_2^{\ell N}$ parameterizations are still constrained by the HERA data. However, these three predictions steadily diverge as E_ν further increases until they differ by 1–2 orders of magnitude at typical UHE values of E_ν, reflecting the different low-x behaviors of the respective parameterizations of $F_2^{\ell N}$.

In summary, we derived a novel concise relationship, given by Eqs. (10)–(12), between the total cross section $\sigma_i^{\nu N}(E_\nu)$ of CC and NC νN DIS in the high-E_ν limit and the structure function $F_2^{\ell N}(x, Q^2)$ in the low-x limit. It is particularly useful for applications to UHE-neutrino physics providing reliable predictions in a very quick and convenient way as it does. Being given in terms of a closed analytic formula, it also allows one to unambiguously determine if $\sigma_i^{\nu N}$ resulting from a given functional form of $F_2^{\ell N}$ satisfies the Froissart bound [9] or not, while this is hardly possible by using the numerical solution of the two-dimensional integral in Eq. (5). Specifically, if $F_2^{\ell N}$ exhibits a low-x behavior $\propto \ln^p(1/x)$, which corresponds to a high-s behavior $\propto \ln^p s$ in Eq. (10), then the coefficient $\tilde{M}$ in that equation produces an additional factor $\propto \ln s$, so that the Froissart bound is violated for $p > 1$. In fact, this is the case for the BBT [6–8] parameterization of $F_2^{\ell N}$, for which $p = 2$. On the other hand, the H [20] one is characterized by $p = 1$, so that the Froissart bound is satisfied.

As expected, the low-x behavior of the PM result for $F_2^{\ell N}$ is too singular for $\sigma_i^{\nu N}$ to satisfy the Froissart bound. It is likely that the inclusion of nonlinear terms, such as screening corrections generated by gluon saturation or recombination, in the evolution equations will cure this problem [10]. In fact, considering the Ayala–Gay-Ducati–Levin [11] and the generalized Golec-Biernat–Wüsthoff [12] models of saturation, where, due to their specific gluon densities, $F_2^{\ell N} \propto Q^2 \ln^p(1/x)$ with $p = 1$ and $p = 0$, respectively, we obtain $\sigma_i^{\nu N} \propto \ln^{p+2} s$, where the second additional logarithm arises from the Q^2 integration in Eq. (9). Thus, saturation strongly modifies the powerlike perturbative asymptotics of total cross sections and has the potential to restore the Froissart bound, as in the case of the Golec-Biernat–Wüsthoff model.

Future measurements of νN DIS with UHE neutrinos will eventually provide direct access to the low-x asymptotic behavior of $F_2^{\ell N}$, far beyond the reach of accelerator experiments, and our new relationship will provide a convenient tool to expose it. On the theoretical side, one important lesson to be learned from our specific example, where total cross sections could be simply related to structure functions in the framework of perturbation theory, is that the direct application of the Froissart bound to structure functions represents a potential pitfall, of which we wish to caution the reader.

We thank Jochen Bartels, Lev Lipatov, and Günter Sigl for useful discussions. This work was supported in part by BMBF Grant No. 05H09GUE, HGF Grant No. HA 101, DFG Grant No. INST 152/465-1, Heisenberg-Landau Grant No. 5, and RFBR Grant No. 10-02-01259-a.

[1] J. K. Becker, Phys. Rep. **458**, 173 (2008).
[2] Yu. M. Andreev, V. S. Berezinsky, and A. Yu. Smirnov, Phys. Lett. **84B**, 247 (1979).
[3] D. W. McKay and J. P. Ralston, Phys. Lett. **167B**, 103 (1986).
[4] R. Gandhi, C. Quigg, M. H. Reno, and I. Sarcevic, Phys. Rev. D **58**, 093009 (1998).
[5] R. Fiore *et al.*, Phys. Rev. D **68**, 093010 (2003).
[6] M. M. Block, E. L. Berger, and C.-I. Tan, Phys. Rev. Lett. **97**, 252003 (2006); E. L. Berger, M. M. Block, and C.-I. Tan, Phys. Rev. Lett. **98**, 242001 (2007).
[7] E. L. Berger, M. M. Block, D. W. McKay, and C.-I. Tan, Phys. Rev. D **77**, 053007 (2008).
[8] M. M. Block, P. Ha, and D. W. McKay, Phys. Rev. D **82**, 077302 (2010).
[9] M. Froissart, Phys. Rev. **123**, 1053 (1961); A. Martin, Phys. Rev. D **80**, 065013 (2009).
[10] M. H. Reno, Nucl. Phys. B, Proc. Suppl. **143**, 407 (2005).
[11] M. B. Gay Ducati and V. P. Goncalves, Phys. Lett. B **502**, 92 (2001).
[12] J. Bartels, K. J. Golec-Biernat, and H. Kowalski, Phys. Rev. D **66**, 014001 (2002).
[13] K. Nakamura *et al.* (Particle Data Group), J. Phys. G **37**, 075021 (2010).
[14] A. V. Kotikov, Phys. Lett. B **338**, 349 (1994).
[15] F. D. Aaron *et al.* (H1 and ZEUS Collaborations), J. High Energy Phys. 01 (2010) 109.
[16] C. Lopez and F. J. Ynduráin, Nucl. Phys. **B171**, 231 (1980); **B183**, 157 (1981).
[17] A. V. Kotikov and G. Parente, Nucl. Phys. **B549**, 242 (1999); A. Yu. Illarionov, A. V. Kotikov, and G. Parente, Phys. Part. Nucl. **39**, 307 (2008).
[18] A. D. Martin, W. J. Stirling, R. S. Thorne, and G. Watt, Eur. Phys. J. C **64**, 653 (2009).
[19] H.-L. Lai *et al.*, Phys. Rev. D **82**, 074024 (2010).
[20] D. Haidt, Nucl. Phys. B, Proc. Suppl. **79**, 186 (1999).